Original Research Article

PMSM Speed Control Using an Enhanced State Feedback Controller and Linear Quadratic Regulator for effective Drive System.

ABSTRACT:—This paper introduced an effective method for regulating and controlling the speed of PMSMs (permanent magnet synchronous motors) by linearizing the non-linear and time-varying equations that model the PMSM. This method was achieved by utilizing an improved state feedback controller along with a linear quadratic regulator (LQR) to determine optimal performance indices. In order to assess external load torque disturbances in the system, a disturbance observer (DO) method was employed. Additionally, a sliding mode observer was utilized in conjunction with the disturbance observer to control motor speed. Simulations were conducted to compare the state feedback controller with a conventional PI- controller. The results showed that the state feedback controller achieved a more robust and improved speed and torque dynamic performance with a reduced steady-state error percentage of 24.17% and 23.51%, compared to the 38.0% and 38.37% obtained using a PI-controller. The derived state feedback matrix (K), based on Ackerman's rule, demonstrated that the entire system is controllable and that the performance index is marginally stable.All simulations were achieved in MATLAB/SIMULINK 2021 version.

Keywords—Permanent Magnet Synchronous Motor, Mathematical modeling, Linear quadratic regulator (LQR), Disturbance Observer (DO), Sliding-Mode-Observer (SMO), PI-Controller, State-Feeedback Controller (SFC), Simulation.

1. INTRODUCTION

Recent advancement in technology has shown that PMSM-motors are currently deployed to different electrical and mechanical use due to their prevailing importance which include high torque to weight ratio, greater efficiency, simplicity in structure, negligible rotor heating, small moment of inertia and low torque ripple [1-2]. The traditional control scheme for PMSM speed is the vector control method which shows that torque angle is kept at $\delta = 90^0$ while ensuring that the reference direct axis current is held at a zero value [3-4]. In recent time, vector control and direct torque regulation in addition to the adaptive sliding mode control are the most recommended processes of speed control [5]. In real life applications, applied load disturbances are unavoidable. Hence, establishing a precise steady state speed control during a distressed state with reduced steady state speed error becomes very expedient to address the regulation approach. Externally applied torque is though seen as a major drawback which affects a steady state speed operation of a permanent magnet synchronous machine (PMSM). The motive of a quality control machine specialist is to regulate or completely reduce the effects of this disturbance on the steady state speed limits. In [6]-[8], detailed work on the various forms of disturbance evaluation techniques was discussed. Parameter variations and incorrect adjustment of speed and machine load-ability has generated a consequential effect on the steady state speed operation. Presently, emphasis is on how to adopt a pragmatic approach in ensuring that during a transient disturbance, a fast-dynamic response is achieved at a shorter time period thereby reducing the risk of heat dissipation and noisy process.

2. LITERATURE REVIEW OF RELATED WORK

Several research works have been carried out on PMSM speed control and regulations with the attendant disturbances. In [9], a problem of stabilization for non-linear delay systems was addressed with exogenous disturbances and event-triggered feedback control. In [10], output feedback stabilization problem with unknown control coefficients and output function was reported. A disturbance estimation is examined on PMSM speed controller using extended state observer (ESO) and was presented in [11-12]. Parameter variation with mismatched uncertainty for non-linear disturbance observer control was applied in the PMSM drive system as reported in [13]. In [14], a predictive control with extended state observer was used in optimizing the PMSM control performance while in [15], control involving a reference model adaptive

control with estimated disturbance was applied in speed regulation for a constrained state feedback. In [16], an extreme sliding mode speed regulation method was presented. In [17], a Sensorless PMSM speed control with disturbance and observer method was realized. In [18], a composite speed controller for PMSM was developed in an uneven disturbance. Fractional order proportional integral controller was developed for the control of the PMSM speed [19]. Controller with dual degree of freedom was adopted for robust speed control. A model predictive speed control applied in speed ripple minimization of the PMSM was detailed in [20]. A novel approach of PMSM speed control system with anti-disturbance sliding mode was also reported in [21].

A current control with disturbance observer for PMSM speed drivesby means of an adaptive sliding mode was presented in [22]. A speed controller design was proposed for PMSM drives using only SMC as presented in [23]. Zhang et al also illustrated a non-linear PMSM speed control with sliding mode and disturbance compensation [24]. Combination of PMSM speed with current for terminal sliding mode control and non-linear disturbance observers was illustrated in [25]. A sliding mode control with non-linear fractional order PID sliding surface for the speed performance of surface mounted PMSM drives based on an extended state observer was presented in [26]. A work on PMSM servo-drive control system state feedback and load torque using feed forward compensation was given in [27]. In [28], a simplified two degrees of freedom for robust speed control of PMSM was reported. It is worthy of note that in all the literature reviewed material, speed control was accomplished with the aid of different controller's design which gave different percentage steady state error value under negative perturbation. New method applied here involves a proximity monitoring of the disturbance in order to readjust the speed operational point which is constantly updated with disturbance-observer method during speed perturbation. The model for permanent magnet synchronous motor is linearized around this operating point while a state feedback controller (SFC) is designed with the updated linearized model obtained from a linear-quadratic regulator (LQR). In addition, an optimal control index was obtained using Ackerman's method and a comparison was drawn from simulation results on cascaded operations based on improved sliding mode with disturbance-observer and a PI-controller's approach. This work is arranged the following: Segment I is the introduction. Segment II reviewed literature of related work. Segment III which is research methodology discussed the PMSM mathematical modeling in non-linear and linear states with the design of an optimal linear quadratic regulator algorithm. Segment IV presents the results of simulation. Segment V the research work is concluded here.

3. RESEARCH METHODOLOGY: PMSM MATHEMATICAL MODELING AND DESIGN OF OPTIMAL LINEAR QUADRATIC REGULATOR.

The mathematical modeling of the PMSM is developed based on the vector control where the axis of rotor rotating flux aligns with d-axis of the machine. It is presumed that inductance is independent of the rotor position. A comprehensive non-linear model for surface mounted PMSM equations are given in (1) – (4) as represented by [29].

$$V_q = R_s i_q + L\frac{di_q}{dt} + \omega_r L i_d + \omega_r \lambda_{af} \quad (1)$$

$$V_d = R_s i_d + L\frac{di_d}{dt} - \omega_r L i_q \quad (2)$$

$$\frac{d\omega_{mr}}{dt} = \frac{1}{J}(T_e - T_L - B\omega_{mr}) \quad (3)$$

$$T_e = \frac{3}{2} \times \frac{P}{2} \times i_q \times (\lambda_{af}) \quad (4)$$

In state space, equations (1)-(4) can be re-arranged to equations (5) – (7)

$$\frac{di_q}{dt} = \frac{V_q}{L} - \frac{R_s}{L} i_q - \omega_r i_d - \frac{\lambda_{af}}{L}\omega_r \quad (5)$$

$$\frac{di_d}{dt} = \frac{V_d}{L} - \frac{R_s}{L} i_d + \omega_r i_q \quad (6)$$

$$\frac{d\omega_{mr}}{dt} = \frac{K_t}{J} i_q - \frac{B}{J}\omega_{mr} - \frac{P}{2 \times J} T_L \quad (7)$$

The mechanical and the electrical speed is related by equation (8).

$$\omega_r = \frac{P}{2}\omega_{mr} \quad (8)$$

Where: $[i_q i_d \omega_{mr}]$ are system states, $[V_q V_d]$ represents inputs of the system. The external disturbance which is given by equation (9) is dependent on the applied load torque T_L.

$$d = -\frac{P}{2J} T_L \quad (9)$$

Figure 1 illustrates the conventional vector outline for the PMSM drive with a Proportional Integral (PI) controller.

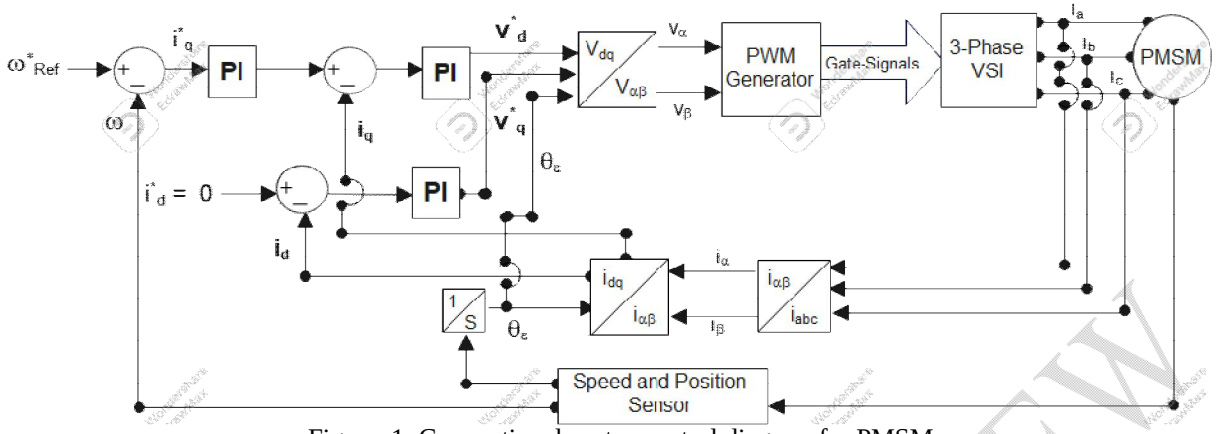

Figure. 1: Conventional vector control diagram for PMSM

A Jacobian linearization method for equations (5) – (8) is presented in equation (10) for a linearized function.

$$\dot{X} = \begin{bmatrix} \frac{-R_s}{L} & -\omega_o & \frac{-(\lambda_{af} + LI_{do})}{L} \\ \omega_o & \frac{-R_s}{L} & i_{qo} \\ \frac{K_t}{J} & 0 & \frac{-B}{J} \end{bmatrix} + \begin{bmatrix} \frac{1}{L} & 0 \\ 0 & \frac{1}{L} \\ 0 & 0 \end{bmatrix} u + \begin{bmatrix} 0 \\ 0 \\ 1 \end{bmatrix} d \quad (10)$$

The model presented in (10) is a PMSM linearized model around an operating point $[i_{qo} i_{do} \omega_{mo}]$. For a vector control, a constant torque angle of $\delta = 90^0$ is required which gives rise to $i_d = 0$ while $i_{qo} = i_q^*$ that varies as the load torque changes. In steady state condition, the load torque is always equivalent to the motor developed torque

$$T_e T_L = T_e \quad (11)$$

Substituting equation (4) into equation (11) while observing the vector control conditions gives rise to equation (12).

$$i_q^* = i_{qo} = \frac{T_L}{\left(\frac{3}{2}\frac{P}{2}\lambda_{af}\right)} \quad (12)$$

Based on equation (12), it is obvious that i_{qo} is dependent on the disturbance and is restored using a disturbance-observer (DO) with a new operating point $[i_{qo} i_{do} \omega_{mo}]$ successfully updated. Two cascade observers which include sliding mode observer and disturbance observer are used for speed estimation and disturbance. Sliding mode is a generally known technique applied in hardware implementation [24-25]. Sliding mode observer is achieved using PMSM equation model based on Clark's αβ coordinate transformation system. Therefore, transforming equations (1) and (2) into αβ coordinate with the back emf incorporated gives rise to equations (13) – (16).

$$L\frac{di_\alpha}{dt} = -Ri_\alpha - e_\alpha + V_\alpha \quad (13)$$

$$L\frac{di_\beta}{dt} = -Ri_\beta - e_\beta + V_\beta \quad (14)$$

$$e_\alpha = -\lambda_{af}\omega_r \sin\theta \quad (15)$$

$$e_\beta = -\lambda_{af}\omega_r \cos\theta \quad (16)$$

Considering Sliding mode variable structure concept, the surface current chosen are presented in (17) – (19).

$$S = \hat{i}_s - i_s \quad (17)$$

$$i_s = [i_\alpha i_\beta] \quad (18)$$

$$\hat{i}_s = [\hat{i}_\alpha \hat{i}_\beta] \quad (19)$$

Where i_α and i_β areαβ stator currents, $\hat{i}_\alpha$ and $\hat{i}_\beta$ are αβ estimated currents. On attaining sliding surface, S is zero while $\hat{i}_\alpha = i_\alpha$and $\hat{i}_\beta = i_\beta$. The observer is therefore robust under this condition. The back emf also changes with the new expression obtained based on the dynamic equations presented in equations (20) and (21).

$$L\frac{d\hat{i}_\alpha}{dt} = -R\hat{i}_\alpha - K_s sgn(\hat{i}_\alpha - i_\alpha) + V_\alpha \quad (20)$$

$$L\frac{d\hat{i}_\beta}{dt} = -R\hat{i}_\beta - K_s sgn(\hat{i}_\beta - i_\beta) + V_\beta \quad (21)$$

Comparing equations (13) and (14) with (20) and (21) gives rise to the emf equation presented in equation (22).

$$\left.\begin{aligned} \hat{e}_\alpha &= K_s sgn(\hat{i}_\alpha - i_\alpha) \\ \hat{e}_\beta &= K_s sgn(\hat{i}_\beta - i_\beta) \end{aligned}\right\} \quad (22)$$

As earlier mentioned, the externally applied load torque is considered as a disturbance. This disturbance is assessed with a designed equation termed as disturbance-observer equation presented in equation (23).

$$\frac{d\omega_{mr}}{dt} = \frac{1}{J}\left(\frac{3}{2}\frac{P}{2}\lambda_{af} i_q - T_L - B\omega_{mr}\right) \quad (23)$$

Selecting state variables $x = \omega_{mr}$, disturbance as $d = \frac{-T_L}{J}$, $K_T = \frac{1}{J}\frac{3}{2}\frac{P}{2}\lambda_{af}$ and rewriting equation (23) gives rise to equation (24).

$$\dot{X} = \frac{-B}{J}X + K_T i_q + d \quad (24)$$

The disturbance is presumed as a gradually changing load torque disturbance which can be compensated with a properly designed controller. A controller is designed based on the linearized model presented in equation (10) which is compactly represented in equation (25).

$$\left.\begin{aligned} \dot{X} &= Ax + B_u U + B_d d \\ Y &= Cx \end{aligned}\right\} \quad (25)$$

Where: $A = \begin{bmatrix} \frac{-R_s}{L} & -\omega_o & \frac{-(\lambda_{af} + LI_{do})}{L} \\ \omega_o & \frac{-R_s}{L} & i_{qo} \\ \frac{K_t}{J} & 0 & \frac{-B}{J} \end{bmatrix}$; $B_u = \begin{bmatrix} \frac{1}{L} & 0 \\ 0 & \frac{1}{L} \\ 0 & 0 \end{bmatrix}$;

$B_d = \begin{bmatrix} 0 \\ 0 \\ 1 \end{bmatrix}$; $C = [0\ 0\ 1]$; $x = [i_q i_d \omega]$; $U = [V_q V_d]^T$. Initial steady-state operating point is given by $x = [i_{qo} i_{do} \omega_o]$. A linear state feedback controller (SFC) meant for tracking the anticipated result is gotten from a Linear-Quadratic Regulator (LQR) Controller. A modified block diagram of Figure 1 with Sliding Mode Observer and Disturbance Observer incorporated is presented in Figure 2.

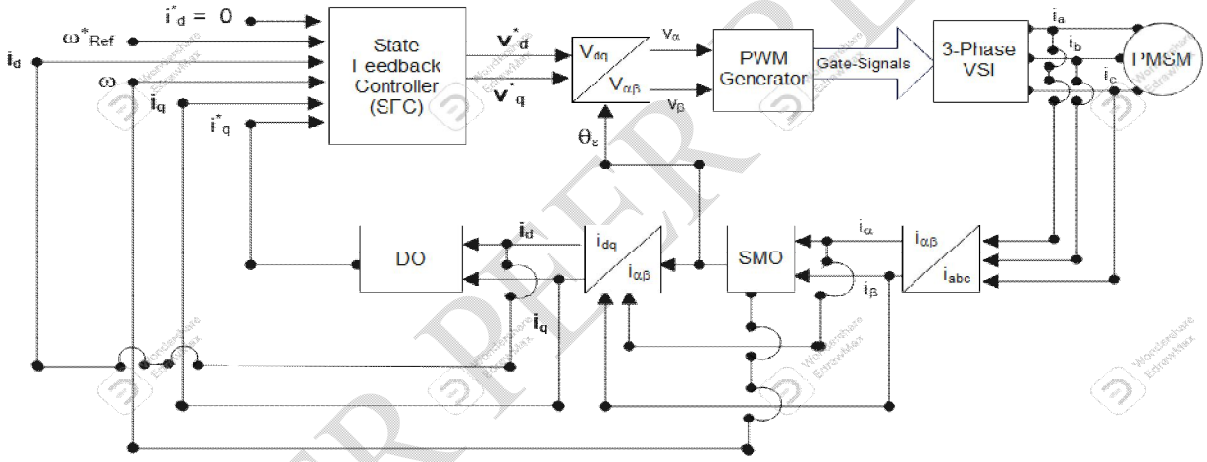

Figure 2: Modified diagram of PMSM vector control with SMO and DO.

A linear quadratic regulator is an optimal control problem where machine state equation is made linear, the cost function is quadratic and the test conditions comprise initial condition on the state with no disturbance input. A conventional state feed controller (SFC) is always designed using state errors. For a design with negligible steady state error in speed, an integral feedback controller is applied as presented in equation (26).

$$U = -Kx(X^* - X) + K_b\zeta_b \quad (26)$$

Where: $\zeta_b = (\omega^* - \omega)$. Augmenting equation (25) and (26) gives rise to equation (27).

$$\begin{bmatrix} \dot{X}_{(t)} \\ \dot{\zeta}_{b(t)} \end{bmatrix} = \begin{bmatrix} A & 0 \\ -C & 0 \end{bmatrix}\begin{bmatrix} x_{(t)} \\ \zeta_{b(t)} \end{bmatrix} + \begin{bmatrix} B \\ 0 \end{bmatrix}U(t) + \begin{bmatrix} B_d \\ 0 \end{bmatrix}d(t) + \begin{bmatrix} B \\ 0 \end{bmatrix}\omega^*(t) \quad (27)$$

When $t = \infty$, equation (27) changes to equation (28) as presented.

$$\begin{bmatrix} \dot{X}_{(\infty)} \\ \dot{\zeta}_{b(\infty)} \end{bmatrix} = \begin{bmatrix} A & 0 \\ -C & 0 \end{bmatrix}\begin{bmatrix} x_{(\infty)} \\ \zeta_{b(\infty)} \end{bmatrix} + \begin{bmatrix} B \\ 0 \end{bmatrix}U(\infty) + \begin{bmatrix} B_d \\ 0 \end{bmatrix}d(\infty) + \begin{bmatrix} B \\ 0 \end{bmatrix}\omega^*(\infty) \quad (28)$$

Subtracting equation (28) from equation (27) gives rise to equation (29).

$$\begin{bmatrix} \dot{X}_{(t)} - \dot{X}_{(\infty)} \\ \dot{\zeta}_{b(t)} - \dot{\zeta}_{b(\infty)} \end{bmatrix} = \begin{bmatrix} A & 0 \\ -C & 0 \end{bmatrix} \begin{bmatrix} x_{(t)} - x_{(\infty)} \\ \zeta_{b(t)} - \zeta_{b(\infty)} \end{bmatrix} + \begin{bmatrix} B \\ 0 \end{bmatrix} U_{(t)} - U_{(\infty)} + \begin{bmatrix} B_d \\ 0 \end{bmatrix} d_{(t)} - d_{(\infty)} + \begin{bmatrix} B \\ 0 \end{bmatrix} \omega^*_{(t)} - \omega^*_{(\infty)} \quad (29)$$

In a compact arrangement, equation (29) can be rewritten as presented in equation (30).

$$\begin{bmatrix} \dot{X}_{e(t)} \\ \dot{\zeta}_{e(t)} \end{bmatrix} = \begin{bmatrix} A & 0 \\ -C & 0 \end{bmatrix} \begin{bmatrix} x_{e(t)} \\ \zeta_{e(t)} \end{bmatrix} + \begin{bmatrix} B \\ 0 \end{bmatrix} U_{e(t)} + \begin{bmatrix} B_d \\ 0 \end{bmatrix} d_{e(t)} + \begin{bmatrix} B \\ 0 \end{bmatrix} \omega^*_{e(t)} \quad (30)$$

Where: $\dot{X}_{e(t)} = \dot{X}_{(t)} - \dot{X}_{(\infty)}$; $\dot{\zeta}_{e(t)} = \dot{\zeta}_{b(t)} - \dot{\zeta}_{b(\infty)}$; $x_{e(t)} = x_{(t)} - x_{(\infty)}$; $\zeta_{e(t)} = \zeta_{b(t)} - \zeta_{b(\infty)}$; $U_{e(t)} = U_{(t)} - U_{(\infty)}$;
$d_{e(t)} = d_{(t)} - d_{(\infty)}$; $\omega^*_{e(t)} = \omega^*_{(t)} - \omega^*_{(\infty)}$.

A relational equation for the control vector $U_{e(t)}$ and the error vector $e(t)$ is defined by equation (31).

$$\dot{e}(t) = \hat{A}e(t) + \hat{B}Ue(t) \quad (31)$$

Where: $\hat{A} = \begin{bmatrix} A & 0 \\ -C & 0 \end{bmatrix}$; $\hat{B} = \begin{bmatrix} B \\ 0 \end{bmatrix}$; $Ue(t) = -Ke(t)$;

$K = \begin{bmatrix} k_x \\ k_b \end{bmatrix}^T$.

The simplified state equation that represents the error vector with the system matrix is presented in equation (32).

$$\dot{e}(t) = (\hat{A} - \hat{B}K)e \quad (32)$$

So, by direct placement of the Eigen vector in equation (32) and by verifying the resultant values through MATLAB, the nature of the stability error $e(t)$ limit is obtained. A linear quadratic regulator generally is intended to curtail a quadratic performance measure of a non-linear equation. A reliable cost function to use when the control system is designed to operate for a long period of time is given by equation (33).

$$J = \frac{1}{2}\int \left(x^T_{(t)} Q x_{(t)} + U^T_{(t)} R U_{(t)}\right) dt \quad (33)$$

In this case, $Q \geq 0$ and $R > 0$ though their values are determined by control Engineer or designers. Q and R values are chosen as unity matrix for accuracy and simplicity.

$Q = \begin{bmatrix} 1 & 0 & 0 \\ 0 & 1 & 0 \\ 0 & 0 & 1 \end{bmatrix}$ and R = 1. The state feedback matrix gain (K) is shown in equation (34). Where P is the solution to the algebraic matrix Riccati equation presented in equation (35).

$$K = R^{-1}B^T P x^T_{(t)} \quad (34)$$

$$PA + A^T P - PBR^{-1}B^T P + Q = 0 \quad (35)$$

The most commonly used approach in determining the value of (P) is built on trial-and-error method. Therefore, substituting the value of the machine parameters in Table 1 into the state system matrix gives rise to a solution to equation (35).

$$PA = \begin{bmatrix} P_{11} & P_{12} & P_{13} \\ P_{12} & P_{22} & P_{23} \\ P_{13} & P_{23} & P_{33} \end{bmatrix} \begin{bmatrix} -100 & -314.2 & -4 \\ 314.2 & -100 & 2 \\ 152.8 & 0 & 0 \end{bmatrix} \text{ and}$$

$$A^T P = \begin{bmatrix} -100 & 314.2 & 152.8 \\ -314.2 & -100 & 0 \\ -4 & 2 & 0 \end{bmatrix} \begin{bmatrix} P_{11} & P_{12} & P_{13} \\ P_{12} & P_{22} & P_{23} \\ P_{13} & P_{23} & P_{33} \end{bmatrix}.$$

Where

$P_{12} = P_{21}$, $P_{23} = P_{32}$, $P_{13} = P_{31}$, $B = \begin{bmatrix} 0 \\ 0 \\ 1 \end{bmatrix}$ and $B^T = [0\ 0\ 1]$. The SFC gain K in equation (34) can be calculated by substituting these matrix variables into the Riccati equation in (35) to solve for P-values but this may result to a complex matrix computation with attendant error. Therefore, a simplified Linear Quadratic Regulator (LQR) algorithm which minimizes theoptimal performance index is presented in Figure 3. This evaluates the SFC gain K with high accuracy in conformity with [30].

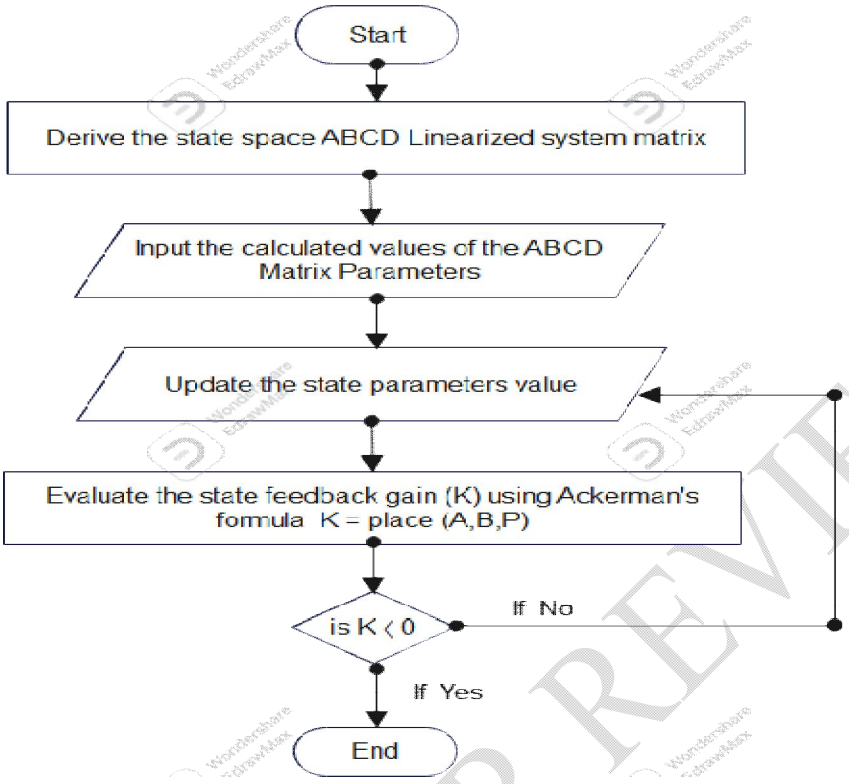

Figure 3: State Feedback gain (K) algorithm with LQR

Table 1: Simulation Parameters used

Parameters	**Values**
Inverter Carrier Frequency (KHz)	5
Modulation index	0.8
PMSM rated power (HP)	15
Supply Frequency (Hz)	50
Rated phase voltage (V)	220
Stator resistance (Ω)	0.875
Inductance (mH)	8.75
Flux linkage (Weber-Turn)	0.0175
d-axis operating current (A)	2
Moment of Inertia (Kgm^2)	0.0875
Viscous friction (N.M.S)	0.00003075
Number of Poles	8
Varying load torque (Nm)	-0.4 and -0.85
Synchronous speed (Rad./Sec.)	78.55
Proportional Controller	1.25
Integral Controller	0.025

4. RESULTS OF SIMULATION AND DISCUSSION.

Table 1 contains the parameters applied in the simulation. In Figure 4, a dq-axes current of the PMSM with state feedback controller is presented while Figure 5 contains dq-axes current with PI-controller. It is obvious in both Figures that the transient response with the PI-controller during an external disturbance is more pronounced than with the SFC controller. This could cause an undesirable noise and vibration in the PMSM. In Figures 6 and 7, rotor speed with SFC controller and PI-controller were presented. It is observed that the speed response

with the SFC controller is very much improved and has a lower percentage steady state error of 24.17% due to reduced settling time of 0.72517 Sec. A synchronous speed of 78.544 Rad/Sec. was also attained at a faster rate with the SFC controllerafter a transient disturbance and under a steady state condition of operation. The speed response to an external disturbance using the PI-controller showed that more ripples were obtained which took a longer duration of 1.13997 Sec. before attaining a steady state condition. This also gave rise to a higher percentage steady state error value of 38.0%. Table 2 shows that an improved dynamic performance is achieved with the SFC controller. In Figures 8 and 9, the electromagnetic torque ripples were reduced using the SFC controller whereas with a PI-controller, an undesirably high oscillation was obtained. The percentage steady state error is expressed as: $\frac{\text{Settling Time (Sec.)}}{\text{Simulation Time (Sec.)}} \times 100$. Therefore, the percentage steady state error in torque as shown in Table 2 indicates that 38.37% was produced with a PI-controller as opposed to 23.51% produced with SFC controller. In Figures 10 and 11, the power outputs of the two controllers were presented. It is also observed that the steady state power output with SFC controller was attained at a faster rate with a settling time of 0.82017 Sec. with a reduced percentage error value of 27.35% as against 38.84% obtained using a PI-controller. In Figures 12 and 13, it is observed that torque-speed characteristics with SFC controller prior to the attainment of synchronous speed value of 78.55 Rad/Sec. exhibited a slight transient characteristic which is less severe as compared with the PI-controller. The inverter phase A gate signal is presented in Figure 14. It is shown in this Figure 14 that IGBT2-Gate signal is complementary to IGBT1-Gate signal and therefore cannot be turned on simultaneously. The inverter phase voltage and current are shown in Figure 15. A close observation shows that the current is almost in phase with the voltage which is indicative of a unity power factor operation. The Eigen values obtained from the algorithm earlier presented in Figure 3 using the state feedback matrix showed that the system equation is controllable with the following values: $\lambda_1 = -99.698 + j315.08$, $\lambda_2 = -99.698 - j315.08$, and $\lambda_3 = -0.6036$. The state feedback gain obtained based on the algorithm presented in Figure 3 is given by

$$K = \begin{bmatrix} 0.0870 & -0.2749 & 0.6219 \\ 0.2749 & -0.0870 & 0.0001 \end{bmatrix} \begin{bmatrix} X_1 \\ X_2 \\ X_3 \end{bmatrix}.$$

The performance control index is therefore minimized by

$$K = \begin{bmatrix} 0.0870X_1 & -0.2749X_2 & 0.6219X_3 \\ 0.2749X_1 & -0.0870X_2 & 0.0001X_3 \end{bmatrix}.$$

Table 2: Performance characteristics of the PMSM based on simulation results.

Varying Parameters	Settling Time (Sec.)	Simulation Time (Sec.)	Steady State error(%) $\frac{\text{Settling Time (Sec.)}}{\text{Simulation Time (Sec.)}} \times 100$
Speed with PID Controller	1.13997	3	38.00
Speed with SFC Controller	0.72517	3	24.17
Electromagnetic Torque with PID Controller	1.15108	3	38.37
Electromagnetic Torque with SFC Controller	0.70508	3	23.51
Power output with PID Controller	1.16536	3	38.84
Power output with SFC Controller	0.820417	3	27.35

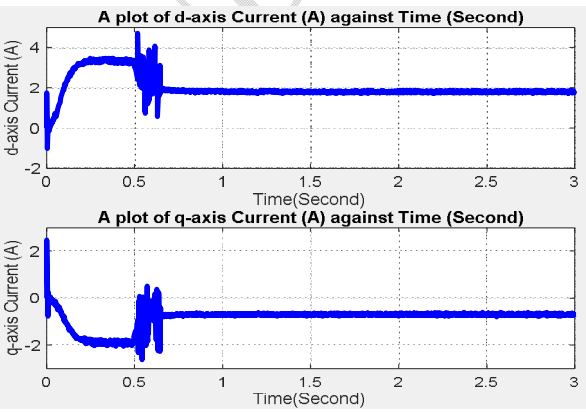

Figure 4: dq-axes Current with SFC-Controller

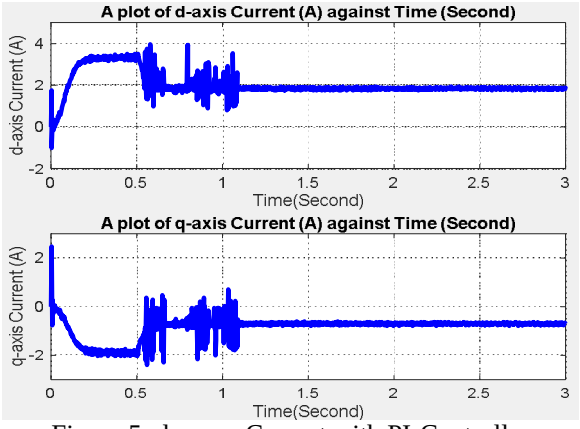

Figure 5: dq-axes Current with PI-Controller

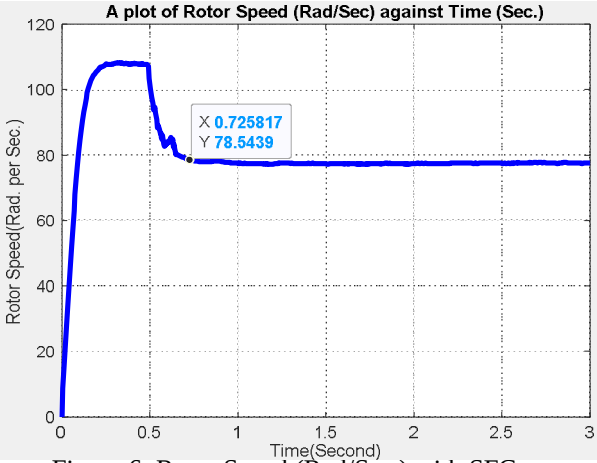

Figure 6: Rotor Speed (Rad/Sec.) with SFC-Controller

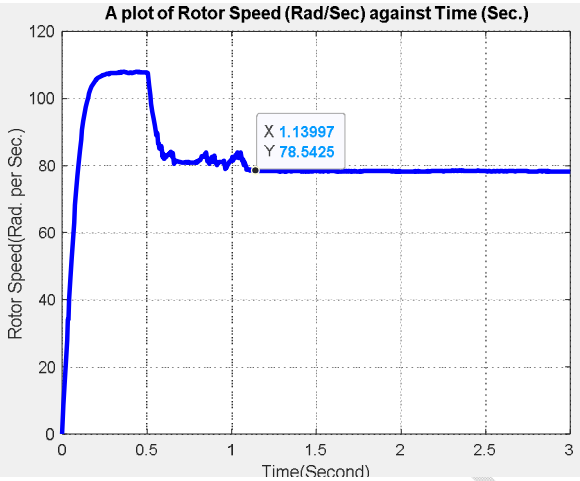

Figure 7: Rotor Speed (Rad/Sec.) with PI-Controller

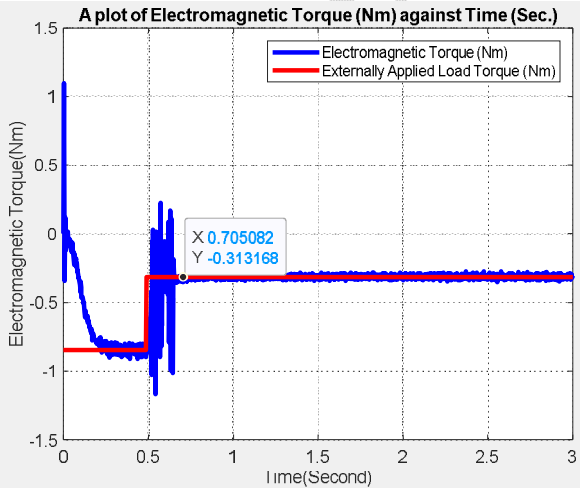

Figure 8: Torque (Nm.) with SFC-Controller

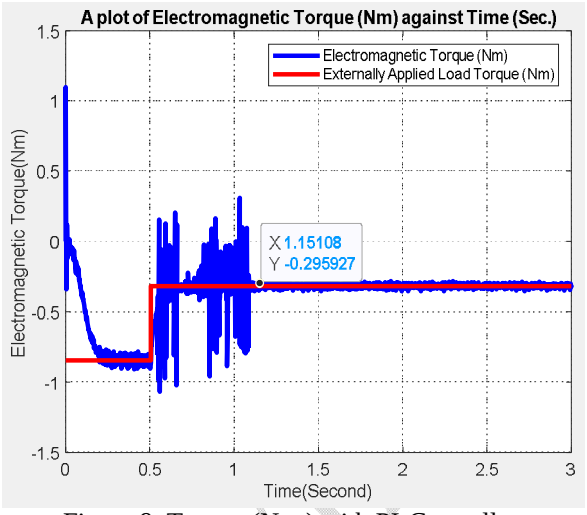

Figure 9: Torque (Nm.) with PI-Controller

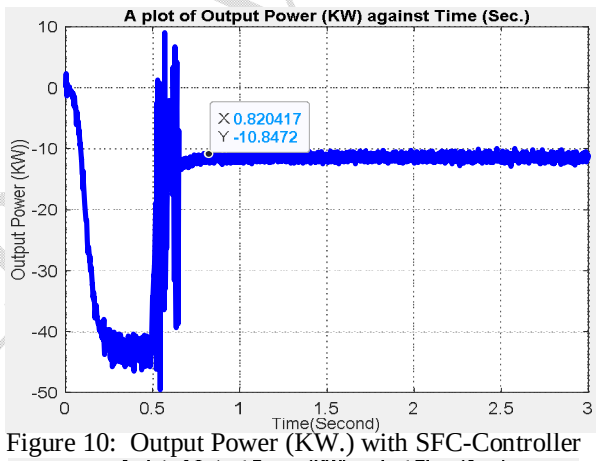

Figure 10: Output Power (KW.) with SFC-Controller

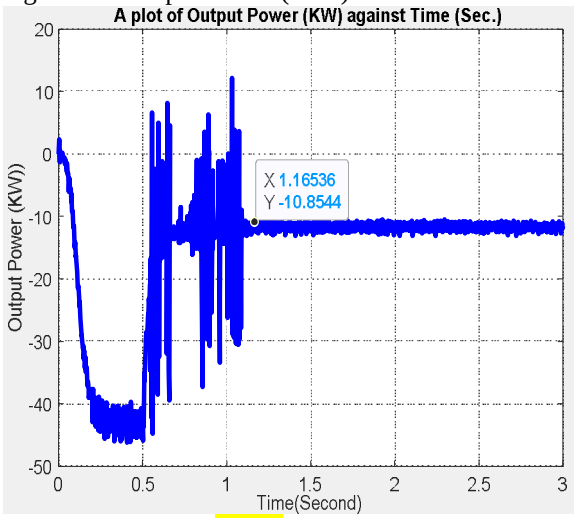

Figure 11: Output Power (KW.) with PI-Controller

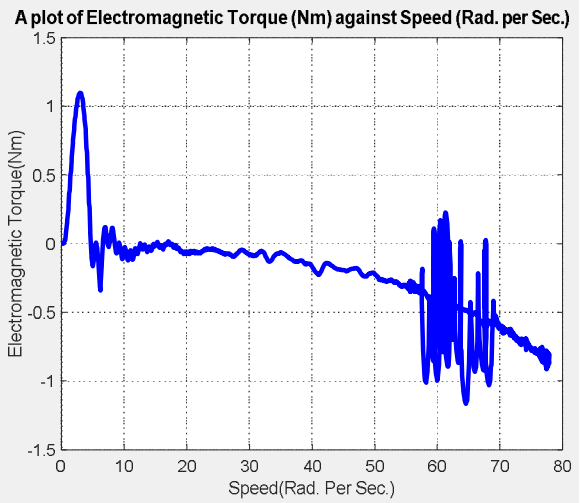

Figure 12: Torque against Speed with SFC-Controller

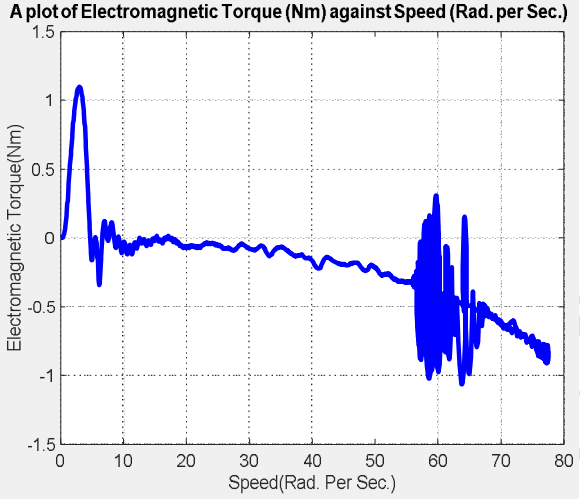

Figure 13: Torque against Speed with PI-Controller

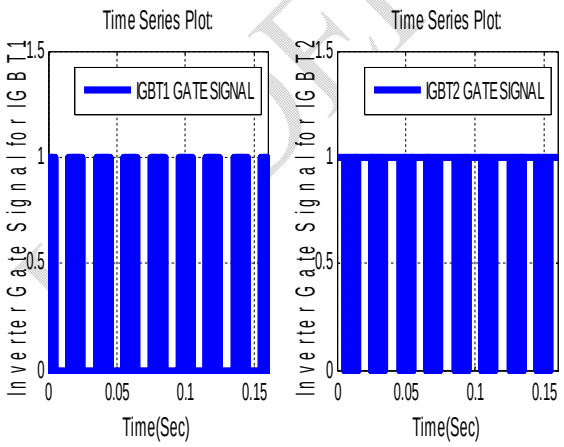

Figure 14: Phase A Inverter Gate Signals

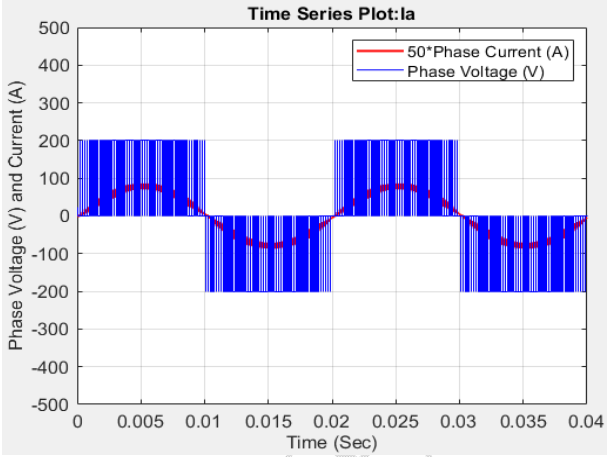

Figure 15: Inverter Phase Voltage (V) and Current (A)

5. CONCLUSIONS.

A non-linear PMSM modeled equation was derived and linearized while a state feedback controller design based on the linearized model was achieved with a linear quadratic regulator (LQR). The state feedback matrix K derived from Ackerman's technique with the computed Eigen values showed that the entire system is controllable and the performance index is marginally stable. The displayed simulation results showed that a substantial enhancement in machine dynamic performance was achieved using a state feedback controller as manifested in the reduced percentage steady state error obtained in the motor speed, electromagnetic torque and power output. In summary, the outcome of this paper proved that SFC controller with a proper parameter selection gave a robust control with good transition time than the traditional PI-Controller.

REFERENCES

[1] Zhang, Y. and Zhu, J. "Direct torque control of permanent magnet synchronous motor with reduced torque ripple and commutation frequency," IEEE Trans. Power Electron, Vol. 26, pp.235-248, 2011.

[2] Ma,Z. Saeidi, S.and Kennel, R. "FPGA Implementation of model predictive control with constant switching frequency for PMSM drives," IEEE Trans. Ind. Informat., Vol. 10, pp. 2055- 2063, 2014.

[3] Krishnan, R. Permanent magnet synchronous and brushless DC motor drives. Boca Raton, Florida USA CRC press, 2010.

[4] Boldea, I. "Control issues in adjustable speed drives," IEEE Ind. Electron.Mag., Vol. 2, no.3, pp. 32-50, Sept. 2008.

[5] Kim, H. Son, J. and Lee, J. "A high-speed sliding mode observer for the Sensorless speed

control of PMSM," IEEE Trans. Ind. Electron., Vol. 58, no.9, pp. 4069-4077, Sept. 2011.

[6] Chen, W.H. Yang, J Guo, L. and S. Li, "Disturbance-observer based control and related methods- An overview," IEEE Trans. Ind. Electron. Vol. 63, no.2, pp. 1083-1095, Feb. 2016.

[7] Li, S. Liu, H.and Ding, S. "A speed control for a PMSM using finite time feedback control and disturbance compensation," Trans. Inst. Measurement control, Vol. 32, no.2, pp. 170-187, 2010.

[8] Li, S. Xia, C. and Zhou, X. "Disturbance rejection control method for permanent magnet synchronous motor speed regulation system," Mechatronics, Vol.22, pp. 706-714, March, 2012.

[9] Zhu, Q. "Stabilization of stochastic non-linear delay systems with exogenous disturbances and the event-triggered feedback control," IEEE Trans Autom. Control, Vol. 64, no. 9, pp. 3764-3771, Sept. 2019.

[10] Zhu, Q. and Wang, H. "Output feedback stabilization of stochastic feed-forward systems with unknown control coefficients and unknown output function," Automatica, Vol. 87, pp.166-175, Jan. 2018.

[11] Liu, H. and Li, S. "Speed control for PMSM servo system using predictive functional control and extended state observer," IEEE Trans. Ind. Electron., Vol. 59, no.2, pp 1171-1183, Feb. 2012.

[12] Xiaoquan, L. Heyian, L. and Junlin, H. "Load disturbance observer-based control method for Sensorless PMSM drive," IET Electr. Power Appl. Vol. 10, no.8, pp. 735-743, 2016.

[13] Yamg, J. Liu, H. Li, S. and Chen, X. "Nonlinear disturbance observer-based control robust tracking control for a PMSM drive subject to mismatched uncertainties," In proc. Chinese control conf. July, 2012, pp. 830-835.

[14] Li, S. Liu, H. and Fu, W. "An improved predictive functional control method with application to PMSM systems," Int. Journal Electron., Vol. 104, no.1 pp. 126-142, 2017.

[15] Tarczewski, T. and Grzesiak, L.M "Constrained state feedback speed control of PMSM based on model predictive approach," IEEE Trans. Industrial Electron., Vol. 63, no.6, pp.3867-3875, June, 2016.

[16] Li, S. Zhou, M. and Yu, X. "Design and implementation of terminal sliding mode control for PMSM speed regulation systems," IEEE Trans. Ind. Inform., Vol.9, no.4, pp.1879-1891, Nov.2013.

[17] Qiao, Z. Shi, T. Tan, Y. Xiu, C. and He, X. "New Sliding mode observer for position Sensorless control of permanent magnet synchronous motor," IEEE Trans. Ind. Electron., Vol 60, no.2, pp. 710-719, Feb., 2013.

[18] Yi, Y. Sun, X. Li, X. and Fan, X. "Disturbance observer based composite speed controller design for trans. Inst. Meas. Control, Vol. 38, no.6, pp. 742-750, 2016.

[19] Apte, A. Thakar, U. and Joshi, V. "Disturbance observer based composite speed control of PMSM using fractional order PI-Controller," IEEE/CAA Journal Autom. Sinica, Vol.6, no.1, pp.316-326, Jan. 2019.

[20] Fei, Q. Deng, Y. Li, H. Liu, J. and Saho, M. "Speed ripple minimization of permanent magnet synchronous motor based on model predictive and iterative learning controls," IEEE Access Vol. 7, pp. 31791-31800, 2019.

[21] Wang, Y. Feng, Y. Zhang, X. and Liang, J. "A new reaching law for ant-disturbance sliding mode control of PMSM speed regulation system," IEEE Trans. Power Electronics, Vol. 35, pp 4117-4126, 2020.

[22] Deng, Y. Wang, J. Li, H. Liu, J. and Tian, D. "Adaptive sliding mode current control with sliding mode disturbance observer for PMSM drives," ISA trans., Vol. 88, pp. 113-126, 2019

[23] Song, Q. and Jia, C. "Robust speed controller design for permanent magnet synchronous motor drives based on sliding mode control," Energia Procedia, Vol. 88, pp 867-873, 2016.

[24] Zhang, X. Sun, L. Zhao, K. and Sun, L. "Nonlinear speed control for PMSM system using sliding mode control and disturbance compensation techniques," IEEE Trans. Power Electron., Vol.28, pp.1358-1365, 2013.

[25] Liu, X. Yu, H. Yu, J. and Zhao, L. "Combined speed and current terminal sliding mode control with nonlinear disturbance observer for PMSM drive," IEEE Access, Vol. 6, pp. 29594-29601, 2018.

[26] Gao, P. Zhang, G. Ouyang, H. and Mei, L. "A sliding mode control with nonlinear fractional order PID sliding surface for the speed operation of surface mounted PMSM drives based on an extended state observer," Math., Problems Eng., Vol. 18, pp.1-3, 2019.

[27] Grzesiak, L.M. Tarczewski, T. (2012). "PMSM servo drive control system with state feedback and load torque feed forward compensation," 15th International Power Electronics and Motion control conference, EPE-PEMC 2012 ECCE Europe, Navi Sad, Serbia.

[28] Mendoza-Mondragon, F. Hernandez-Guzman, V.M. and Rodriguez-Resendiz. J. "Robust speed control of permanent magnet synchronous motors using two degrees of freedom control," IEEE Trans. Ind. Electron., Vol. 65, no.8, pp. 6099-6108, Aug. 2018.
[29] Xu, W.J. "Permanent magnet synchronous motors with linear quadratic speed controller," Energy Procedia, Vol. 14, pp 364-369, 2012.
[30] Molavi, R. and Khaburi, D.A "Optimal control strategies for speed control of permanent magnet synchronous motor drives," International Journal of Electrical and Computer Engineering, Vol.2, no.8, 2008.